Quantitative Structure–Property Relationships for Longitudinal, Transverse, and Molecular Static Polarizabilities in Polyynes

ARTICLE *in* THE JOURNAL OF PHYSICAL CHEMISTRY B · JULY 2009

Impact Factor: 3.3 · DOI: 10.1021/jp904002v · Source: PubMed

2 AUTHORS, INCLUDING:

Constantinos D. Zeinalipour-Yazdi
University College London
30 PUBLICATIONS **293** CITATIONS

SEE PROFILE

Quantitative Structure−Property Relationships for Longitudinal, Transverse, and Molecular Static Polarizabilities in Polyynes

Constantinos D. Zeinalipour-Yazdi*,†,‡ and David P. Pullman‡

Department of Chemistry and Biochemistry, University of California San Diego, San Diego, California 92093, and Department of Chemistry, San Diego State University, San Diego, California 92182

Received: January 12, 2008; Revised Manuscript Received: April 13, 2008

The present work reports for the first time quantitative structure−property relationships, derived at the benchmark CCSD(T)/cc-PVTZ level of theory that estimate the static longitudinal, transverse, and molecular polarizability in polyynes ($C_{2n}H_2$), as a function of their length (L). In the case of independent electron models, regardless of the form of the nuclei potential that the electrons experience, the polarizability increases strongly with system size, scaling as L^4. In contrast, the static longitudinal polarizability in polyynes have a considerably weaker length-dependence ($L^{1.64}$). This is shown to predominantly arise from electron−electron repulsion rather than electron correlation by a systematic study of the polarizability length dependence in several simple quantum mechanical systems (e.g., particle-in-box, simple harmonic oscillator) and other molecular systems (e.g., H_2, H_2^+, polyynes). Decrease of the electron−electron repulsion term is suggested to be the key factor in enhancing nonlinear polarizability characteristics of linear oligomeric and polymeric materials.

Introduction

A fundamental understanding of polarizability at a molecular orbital level can aid in the design and analysis of molecular systems that are held together by $\pi-\pi$ interactions. Molecular polarizabilities determine the strength of interaction between nonpolar molecules, as described by the London[1] equation. We have recently shown that, for $\pi-\pi$ interactions between polycyclic aromatic hydrocarbons (PAHs), there is a linear correlation between the binding energy and the static molecular polarizability.[2,3] Being able to compute the molecular polarizability from simplified relationships that correlate the molecular size to the molecular polarizability can prove very useful in quantifying these interactions and find applications in material coatings. Furthermore, the molecular polarizability is a physical parameter that is invoked very frequently in the description of a wide range of physical phenomena, such as the interaction of photons[4] and particles with molecules[5] as well as other molecular properties such as the bond dissociation energy[6], nonlinear optical properties,[7] hardness/softness[8] and electronegativity.[9] More importantly, conjugated polymers (e.g., polyenes, polyacenes, polyynes) with delocalized electronic π-states constitute an important class of materials that exhibit nonlinear optical properties. Accurate prediction of the polarizability in long-chain conjugated polymers may aid to the molecular engineering of optically active compounds with high specific linear and nonlinear response in the presence of electric fields.[10] In particular, the polarizability of a material is intimately related to the refractive index,[11] which is a critical parameter in the design of planar polymer waveguides,[12] found in applications such as thermal optical switches[13] (TOSs), variable optical attenuators[13] (VOAs), optical couplers/splitters,[14] and arrayed waveguide gratings[15] (AWGs). Thus, many computational studies have attempted to evaluate the polarizability length dependence in linear oligomeric[16–18] and polymeric[19] conjugated-π systems.

Several authors[20] report *ab initio* computations of static polarizabilities (α_{xx}) and first hyperpolarizabilities (γ_{xxx}) of small molecular weight (MW) π-conjugated molecules, such as polyenes, polyynes, and comulenes. Maroulis et al.[21] examined polyynes $C_{2n}H_2$ ($n \leq 4$) and showed that the longitudinal static polarizability and second hyper-polarizability exhibit an $L^{1.5}$ and $L^{3.0}$ (L = molecular length) length dependence, respectively. Archibond et al.[22] using the finite field method and after studying the effects of basis set size on the computed (hyper)polarizabilities suggest $\alpha_{xx}/n = 110 \pm 10$ au and $\gamma_{xxx}/n = (1.0 \pm 0.3) \times 10^{-3}$ au as the infinite chain limit for the longitudinal static polarizability and first hyperpolarizability in polyynes, respectively. Other studies have focused on the effect of the π-bonding sequence[23] in the linear π-conjugated molecules on the (hyper-)polarizability or even the effect of electron donating−withdrawing functional groups[24] terminating the linear chains. Champagne et al.[25] showed that density functional theory (DFT)-based exchange functionals, such as the Becke and the Slater, significantly overestimate the static polarizability. Therefore, some studies have concentrated in finding ways of correcting the polarizability overshooting that conventional DFT computations have exhibited.[26,27] The same authors were able to assess the Young modulus, the force constants, the vibrational frequencies, and the phonon dispersion curves for linear polyynes.[28] Other research efforts focused on methodologies that can be applied to infinite periodic systems[29,26,30] and were successfully applied to quasi-one-dimensional molecule chains of molecular hydrogen.[31]

An important class of linear polymeric material that exhibit π-conjugation are end-capped polyynes ($XC_{2n}X'$ where X, X′ = hydrogen and various organic and organometallic compounds), which have attracted increasing interest because their significant polarizabilities, hyperpolarizabilities, and current−voltage characteristics that make them potential candidates as materials in nonlinear optics and molecular electronic devices.[32] In addition, progress in developing methodologies for synthesizing polyynes has allowed a number of derivatives to be available

* Corresponding author. Current address: University of Cyprus, Department of Chemistry, 75 Kallipoleos St., P.O. Box 20537, 1678 Nicosia, Cyprus. E-mail address: zeinalip@ucy.ac.cy.
† University of California San Diego.
‡ San Diego State University.

10.1021/jp800302s CCC: $40.75
Published on Web 06/04/2008

in sufficient quantity for their study. Recent synthetic methodologies[33] allow the synthesis of long-chain polyynes ($C_{2n}TIPS_2$, $n \leq 10$, TIPS = triisopropylsilyl) that appear to have some unusual optical properties that are length dependent. In particular, the authors show that no saturation of the second hyperpolarizability occurs for $n \leq 10$, and that the power dependence of γ ($L^{4.28}$) is much greater than that of polyenes or polyenynes. Furthermore, the end groups have a significant effect on the physical properties of polyynes since their electron-donating or electron-withdrawing character can affect the polarizability and higher hyperpolarizability of the π-framework.[34] Electron correlation and careful choice of molecular geometry can lead to significant variations in the predicted hyperpolarizabilities of *p*-nitroaniline,[35] polyacetylenes (PAs), and polyynes.[36] Furthermore, Dalskov et al.[37] have performed polarizability calculations for polyynes as large as $C_{100}H_2$ using the uncorrelated random phase approximation (RPA) and the correlated second-order polarization propagator approximation (SOPPA) using fixed bond lengths for the triple (1.18 Å) and single (1.40 Å) carbon−carbon bonds. They observe a converging trend of the static longitudinal polarizability difference ($\Delta\alpha_{zz} = \alpha_{zz}^{n} - \alpha_{zz}^{n-1}$) for $n \geq 9$.

In this study, we explore the polarizability length-dependence in linear polyynes ($C_{2n}H_2$, $n \leq 9$). Polyynes are the simplest molecular system, with respect to their molecular structure, that exhibit π-conjugation. These molecules are one-dimensional, with alternating single and triple bonds between carbon atoms, and their polarizabilities can be computed very accurately for a fairly wide range of lengths because of their high symmetry point group ($D_{\infty h}$). In particular, to minimize potential artifacts in the polarizabilities due to an inadequate level of theory or basis set size, the polyyne geometries were optimized at the benchmark CCSD(T)/cc-pVTZ level (occasionally checked against aug-cc-pVTZ and cc-pVQZ basis sets), and then polarizabilities were computed at the optimized geometries at several levels of theory (RHF, MP2, SCS-MP2, CCSD, CCSD(T), and DFT with B3LYP and PBE) using again the cc-pVTZ basis set (occasionally checked against aug-cc-pVTZ and cc-pVQZ basis sets). Furthermore, the length dependence is studied in three model one-dimensional systems: an electron-in-a-box, an electron undergoing harmonic motion, and an electron-in-a-box with a sinusoidal nuclei potential. Since the size dependence of the polyyne polarizabilities differs significantly from that of the three simplistic models, we seek an explanation of this phenomenon by systematically studying the polarizabilities of H_2^+ and H_2 as a function of internuclear distance and by analyzing the distortion of individual molecular orbitals, in C_8H_2 and the particle-in-a-box (PIB) in the presence of a uniform external electric field.

Computational Methods

The finite-field method[38] was used to compute the polarizability parallel (longitudinal) and perpendicular (transverse) to the molecular axis of the polyynes, H_2^+ and H_2. In this method, a molecule's energy is computed at a series of applied electric fields, and the static polarizabilities are determined from the derivatives of the energy with respect to electric field, at zero field. If the electric field $\varepsilon_{||}$ is applied along the molecular axis, then a Taylor series expansion of the energy E about $\varepsilon_{||} = 0$ gives

$$E = E^{(0)} + \left(\frac{dE}{d\varepsilon_{||}}\right)_0 \varepsilon_{||} + \frac{1}{2}\left(\frac{d^2E}{d\varepsilon_{||}}\right)_0 \varepsilon_{||} + \frac{1}{6}\left(\frac{d^3E}{d\varepsilon_{||}}\right)_0 \varepsilon_{||} + \frac{1}{24}\left(\frac{d^4E}{d\varepsilon_{||}}\right)_0 \varepsilon_{||} + \cdots \quad (1)$$

$$= E^{(0)} - \mu_{||}\varepsilon_{||} - \frac{1}{2}\alpha_{||}\varepsilon_{||} - \frac{1}{6}\beta_{||}\varepsilon_{||} - \frac{1}{24}\gamma_{||}\varepsilon_{||} + \cdots$$

Thus, the static longitudinal and transverse polarizability are defined as

$$\alpha_{||} = -\left(\frac{d^2E}{d\varepsilon_{||}}\right)_0 \quad (2)$$

and

$$\alpha_{\perp} = -\left(\frac{d^2E}{d\varepsilon_{\perp}}\right)_0 \quad (3)$$

respectively.

Note that for centro-symmetric molecules such as the polyynes ($C_{2n}H_2$), odd order terms in the energy expansions are zero by symmetry. Thus only even ordered terms are evaluated in order to obtain the longitudinal and transverse polarizabilities.

The molecular polarizability is very sensitive to molecular geometry, particularly on the degree of bond length alternation, thus all polyynes were first optimized at a very high level of theory, CCSD(T), and with a relatively large basis set, Dunning's correlation-consistent polarized valence triple-ζ (cc-pVTZ) basis set.[39] Optimizations were performed using the numerical optimization capability of the software packages Molpro 2006.1[40] and Gaussian 03.[41] The default of allowing valence, but not core, electron correlation was used. Convergence of the bond lengths with respect to basis set was tested for the smaller MW polyynes (C_2H_2, C_4H_2, C_6H_2, and C_8H_2), using larger basis sets, such as the aug-cc-pVTZ and aug-cc-pVQZ. The effect of an applied electric field (0.004 au, highest field strength used) on the equilibrium structure geometries was also briefly investigated for the smaller MW polyynes, at the CCSD(T)/cc-pVTZ level of theory. No evidence of molecular structure distortion at this electric field strength could be observed.

Polarizabilities at the CCSD(T)/cc-pVTZ optimized geometries were then computed for C_2H_2 through $C_{18}H_2$ using a range of theory levels, including RHF, MP2, SCS-MP2 (ref 42), CCSD, and CCSD(T) as well as DFT with the B3LYP and PBE exchange-correlation functionals. The electric fields strengths used in the finite-field computations were 0, 0.002, and 0.004 au (1 au = 5.14×10^{11} V/m). To ensure that higher order terms in eq 1 are unimportant at these electric field strengths, a number of polarizability computations were also performed at fields 1 order of magnitude smaller, i.e., 0, 0.0002, and 0.0004 au to ensure agreement with the results obtained at larger electric fields.

For the PIB system in which the potential energy varied sinusoidally inside the box, energies and wave functions were determined numerically as a function of electric field by solving the Schrödinger equation with the "shooting" method.[43] A dedicated program written in Maple 9 was developed for this purpose.[44]

Results and Discussion

The presentation of our results is given in the following order: First we present the polarizability trends as a function of length (L) of various simple quantum mechanical systems that lack

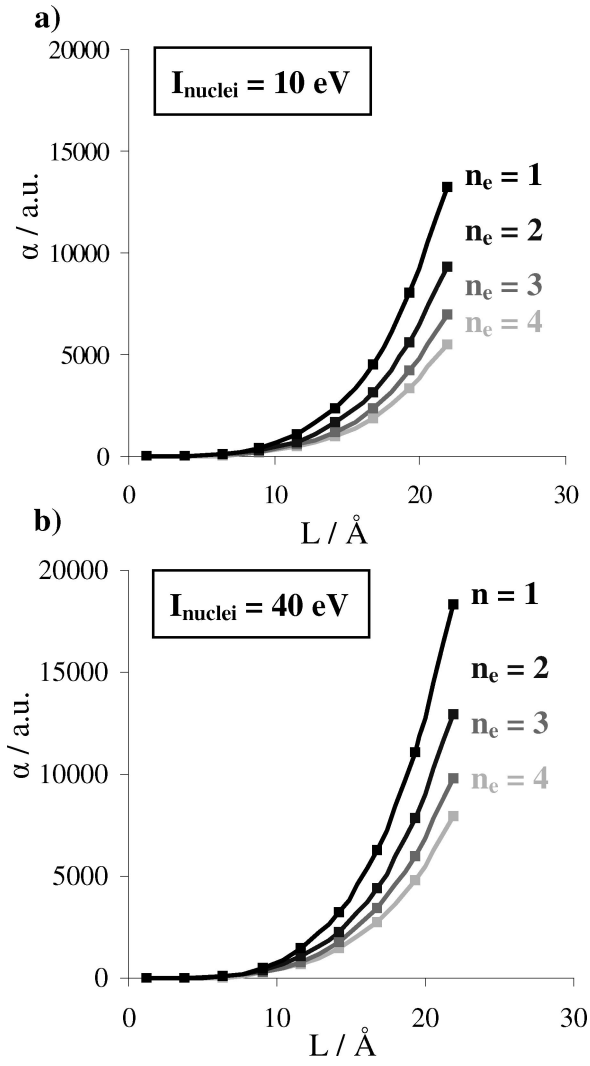

Figure 1. Static longitudinal numerical polarizabilities of 1D-PIB with sinusoidal potential amplitudes of 10 and 40 eV as a function of box length (L).

electron−electron repulsion, such as the one-dimensional particle-in-box (1D-PIB), the one-dimensional simple harmonic oscillator (1D-SHO), the 1D-PIB under the influence of a sinusoidal potential, and the molecular hydrogen cation (H_2^+). Then we compare them to the polarizability of the homologous molecular sequence of linear polyynes $C_{2n}H_2$ ($n \leq 9$) and discuss the trends observed.

A. Simplified Quantum Mechanical Model Systems. ***(i) Analytic Polarizability of 1D-PIB.*** The Schrödinger equation for a particle in a 1D-PIB subjected to a uniform electric field ε can be solved either exactly, with the wave functions expressed in terms of Airy functions,[45,46] or more simply via perturbation theory.[45,47] Our results show that the approximate treatment of second-order perturbation theory is sufficient to yield results as good as the exact numerical solutions. We observe that, as long as the perturbations studied are small, which is achieved by a small external electric field strength, the two methods yield comparable results. In either case, the polarizability is given by eq 2. If the particle is an electron and the potential energy operator is $\hat{V} = \hat{\mu}_x \cdot \hat{\varepsilon} = -e \cdot \varepsilon \cdot x$, the polarizability of the electron in state n is derived in the Appendix and given by

$$\alpha_{xx} = \frac{64e^2 m_e n^2 L^4}{\pi^6 \hbar^2} \sum_{k \neq n} \frac{k^2[(-1)^{n+k} - 1]^2}{(k^2 - n^2)^5} \quad (4)$$

Here, m_e is the electron mass, L is the length of the box, $\hbar$ is Planck's constant divided by 2π, e is the elementary charge of an electron, and n and k are the quantum numbers of the nth and kth energy states, respectively. As shown in eq 4, the polarizability scales as the fourth power of the length for any state n, which is in agreement with the equation-derived polarizability length-dependence by Rustagi et al.[48] The interesting feature of the 1D-PIB and polyyne polarizability calculations is that comparison of their wave functions shows great similarity, nonetheless their polarizability length dependence scales very differently: L^4 and $L^{1.64}$, respectively, as shown in the subsequent sections.

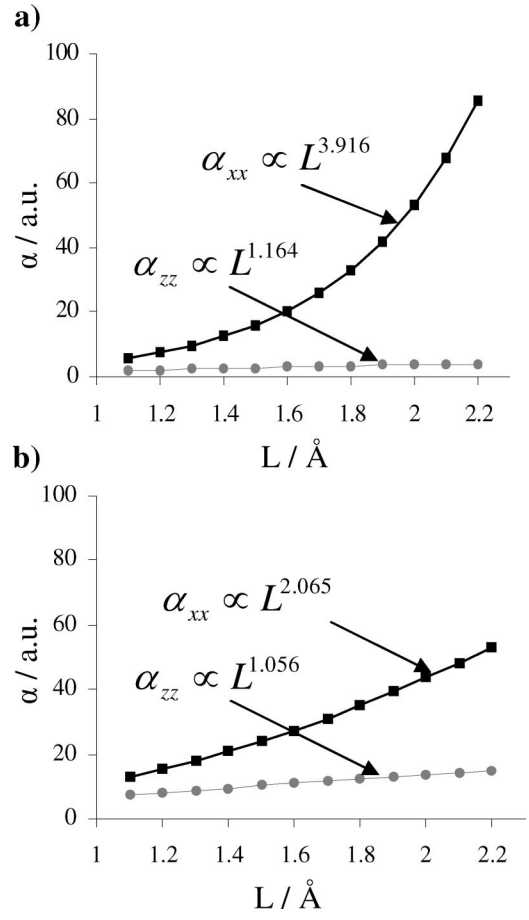

Figure 2. Static polarizability of molecular hydrogen cation (H_2^+) and molecular hydrogen (H_2) as a function of the internuclear hydrogen−hydrogen distance (L). Calculation was carried out at UHF/aug-cc-pVQZ level theory.

TABLE 1: Restricted Hartree−Fock (RHF) Optimized Molecular Geometries of $C_{10}H_2$ Using Various Basis Sets[b]

labels[a]	ccpVDZ	augccpVDZ	ccpVTZ	augccpVTZ	augccpVQZ
r(H−C$_1$)	1.064	1.062	1.054	1.054	1.054
r(C$_1$≡C$_2$)	1.194	1.194	1.183	1.183	1.182
r(C$_2$−C$_3$)	1.386	1.385	1.379	1.379	1.380
r(C$_3$≡C$_4$)	1.198	1.197	1.186	1.186	1.186
r(C$_4$−C$_5$)	1.381	1.380	1.374	1.375	1.375
r(C$_5$≡C$_6$)	1.199	1.198	1.187	1.187	1.187

[a] All values are given in angstroms. [b] Numbering scheme of the carbon atoms in $C_{10}H_2$: H−C$_1$≡C$_2$−C$_3$≡C$_4$−C$_5$≡C$_6$−C$_7$≡C$_8$−C$_9$≡C$_{10}$−H.

TABLE 2: Optimized CCSD(T)/cc-pVTZ Bond Lengths of the Homologous Molecular Sequence $C_{2n}H_2$

labels[a]	C_2H_2	C_4H_2	C_6H_2	C_8H_2	$C_{10}H_2$	$C_{12}H_2$	$C_{14}H_2$	$C_{16}H_2$	$C_{18}H_2$	$C_\infty H_2$
$r(H-C_1)$	1.0637 (1.059)	1.0639 (1.062)	1.0640	1.0642	1.0643	1.0643	1.0644	1.0644	1.0644	
$r(C_1\equiv C_2)$	1.2097 (1.209)	1.2150 (1.206)	1.2165	1.2169	1.2171	1.2171	1.2171	1.2172	1.2172	
$r(C_2-C_3)$		1.3789 (1.380)	1.3725	1.3707	1.3701	1.3698	1.3696	1.3696	1.3696	
$r(C_3\equiv C_4)$			1.2219	1.2240	1.2247	1.2249	1.2250	1.2251	1.2251	
$r(C_4-C_5)$				1.3647	1.3626	1.3617	1.3613	1.3611	1.3610	
$r(C_5\equiv C_6)$					1.2263	1.2271	1.2274	1.2276	1.2276	
$r(C_6-C_7)$						1.3601	1.3592	1.3588	1.3586	
$r(C_7\equiv C_8)$							1.2280	1.2283	1.2285	
$r(C_8-C_9)$								1.3583	1.3578	
$r(C_9\equiv C_{10})$									1.2287	
L	1.2097	3.8089	6.3998	8.9878	11.5750	14.1614	16.7474	19.3334	21.9191	
$\Delta\delta_{mid}$		0.1639	0.1505	0.1407	0.1363	0.1330	0.1313	0.1299	0.1291	0.1276
$\Delta\delta_{end}$		0.1639	0.1560	0.1537	0.1530	0.1526	0.1525	0.1524	0.1523	0.1523

[a] L is the distance between terminal carbon atoms, and $\Delta\delta_{mid}$ and $\Delta\delta_{end}$ are the bond length alternation in the middle and at the ends of the polyynes, respectively. All distances are in angstroms. Values of $\Delta\delta_{mid}$ and $\Delta\delta_{end}$ extrapolated to the infinite chain are given in the final column by fitting with a function of the form $y = a + b\cdot r^x$ and subsequently setting x to infinity. Values in parentheses are the corresponding experimental gas phase bond lengths taken from refs 52 and 53 for C_2H_2 and C_4H_2, respectively. Numbering scheme of the carbon atoms in the polyyne, illustrated for $C_{18}H_2$: $H-C_1\equiv C_2-C_3\equiv C_4-C_5\equiv C_6-C_7\equiv C_8-C_9\equiv C_{10}-C_{11}\equiv C_{12}-C_{13}\equiv C_{14}-C_{15}\equiv C_{16}-C_{17}\equiv C_{18}-H$.

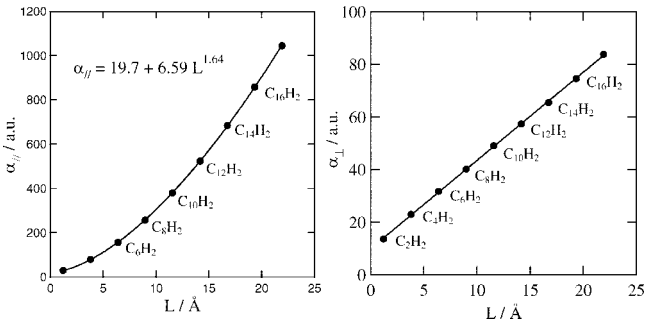

Figure 3. Static (a) longitudinal and (b) transverse polarizability of polyynes ($C_{2n}H_2$, $n \leq 9$) as a function of molecular length (L). Calculation carried out at the CCSD(T)/cc-pVTZ//CCSD(T)/cc-pVTZ level of theory. A polarizability of 1 au is equal to 1.648778×10^{-41} C^2m^2/J.

(ii) Analytic Polarizability of 1D-SHO. The Schrödinger equation for an electron bound harmonically to a positive charge and subjected to an electric field has an analytical solution.[47] The result is that the energy of all harmonic oscillator states are shifted down by $e^2\varepsilon^2/(2k)$, where k is the force constant, thus the polarizability is $\alpha = e^2/k$. To express the polarizability in terms of an extent of motion, we take the "length" L of the oscillator as twice the classical turning point, x_{tp}. One can show that

$$\alpha = \frac{m_e e^2 L^4}{\hbar^2(\nu + \frac{1}{2})^2} \tag{5}$$

where m_e is the mass of the electron, and ν is the quantum number. Thus, as in the PIB case, the polarizability scales again with the fourth power of distance.

(iii) Numerical Polarizability of 1D-PIB with Sinusoidal Potential. The third model system considered is a modified 1D-PIB in which the potential inside the box varies sinusoidally with position. This modification was made to approximately mimic the Coulombic potential an electron experiences due to the nuclei in polyynes. Since the wavelength (λ) of the sinusoidal nuclei potential is constant, effects due to bond length alternations are not monitored. The potential inside the box is given by

$$\hat{V} = A \cdot \sin\left[\frac{2\pi}{\lambda}(x+\phi)\right] - e \cdot \varepsilon \cdot x \tag{6}$$

where A, λ, and φ are the amplitude, period, and phase of the potential, respectively. The Schrödinger equation with such a potential does not have an analytical solution; therefore, wave functions and energies were determined numerically via the "shooting" method[43] (see Appendix) using a devoted computer program written in Maple.[44]

In order to examine the effect of the nuclei potential onto polarizability of the 1D-PIB, we evaluated the polarizability systems that contained as many as four electrons ($n_e = 4$). In Figure 1 we show the static longitudinal numerical polarizabilities 1D-PIB with sinusoidal nuclei potential amplitudes of 10 and 40 eV as a function of box length (L). The results here clearly indicate that introduction of the sinusoidal potential generally increases the polarizability of a quantum system. For a nuclei amplitude of 10 eV, the increase is typically 2−3% compared to the value obtained for the simple 1D-PIB, while, for an amplitude of 40 eV, the increase is as large as 40% in some cases. From these results we expect that, for polyynes, the increase in polarizability due to the potential of the nuclei will be 2−3%, since the actual nuclei potential the electrons feel in conjugated π-systems based on the ionization potential[49] (IP) of ethylene (12.2 eV) and acetylene (12.3 eV) is on the order of 10 eV. Fitting of a power function of the form $y = \mathbf{a}\cdot x^{\mathbf{b}}$ yielded $\mathbf{b} = 4$ for all curves and an $\mathbf{a}$ that roughly linearly decreases with the number of electrons in the system (n). The scaling of the polarizability with system size is essentially L^4, similar to the 1D-PIB and the 1D-SHO cases. These results suggest in general that the nuclei potential generates regions of space along the molecular chain that electrons density can access more easily. This enhances the flow or polarization of electron density along the molecular chain.

(iv) Polarizability of H_2^+ and H_2. The molecular hydrogen cation (H_2^+) is one of the few molecular systems where electron−electron repulsions are absent. Thus, the Hartree−Fock method is sufficient to yield accurate results, and basis set saturation is relatively computationally inexpensive. The one-electron wave function of H_2^+ was expanded within the aug-cc-pVQZ basis with the use 114 primitive gaussians to ensure near basis set saturation. We evaluated the second derivative of the energy with respect to the electric field to obtain the longitudinal and transverse polarizabilities, α_{xx} and α_{zz}, respectively (Figure 2).

The static polarizability of the molecular hydrogen cation scales as $L^{3.9}$, in very close agreement with the L^4 dependence of the simple quantum mechanical systems that lack electron−electron repulsion (1D-PIB, 1D-SHO). The small difference

TABLE 3: Comparison of the Static (a) Longitudinal ($\alpha_{//}$) and (b) Transverse ($\alpha_{\perp}$) Polarizability in Polyynes ($C_{2n}H_2$, $n \leq 9$) Computed Using CCSD(T)/cc-pVTZ//CCSD(T)/cc-pVTZ to Other *Ab Initio* and DFT Methods[a]

(a)	L/Å	$\alpha_{//}$/au CCSD(T)	% diff RHF	% diff MP2	% diff SCS-MP2	% diff CCSD	% diff B3LYP	% diff PBE
C_2H_2	2.2861	29.5	4.2	−1.1	−0.9	−0.4	3.6	3.5
C_4H_2	7.1977	79.6	4.0	−0.3	−1.3	−1.7	8.9	10.7
C_6H_2	12.0939	155.7	3.2	0.6	−2.0	−3.0	14.3	18.2
C_8H_2	16.9845	256.6	2.4	1.7	−1.5	−4.3	19.4	25.7
$C_{10}H_2$	21.8736	380.0	1.5	2.8	−1.4	−5.5	24.6	33.3
$C_{12}H_2$	26.7611	523.6	0.6	3.9	−1.4	−6.6	29.6	41.0
$C_{14}H_2$	31.6481	684.0	−0.2	4.7	−1.5	−7.6	34.7	48.9
$C_{16}H_2$	36.5348	858.0	−0.9	5.5	−1.5	−8.5	39.8	57.0
$C_{18}H_2$	41.4211	1044.8	−1.7	6.2	−1.6	−9.4	44.6	65.1
(b)	L/Å	$\alpha_{\perp}$/au CCSD(T)	% diff RHF	% diff MP2	% diff SCS-MP2	% diff CCSD	% diff B3LYP	% diff PBE
C_2H_2	2.2861	13.7	3.1	−1.4	−1.4	−0.2	3.1	3.9
C_4H_2	7.1977	23.0	2.9	5.5	5.5	−1.1	2.3	2.9
C_6H_2	12.0939	31.7	4.1	1.1	−6.8	−0.1	3.3	3.6
C_8H_2	16.9845	40.2	5.5	2.3	2.3	−0.1	4.4	4.7
$C_{10}H_2$	21.8736	49.1	5.3	0.6	0.5	−0.1	4.1	4.4
$C_{12}H_2$	26.7611	57.4	6.2	2.3	1.2	−0.0	4.9	5.1
$C_{14}H_2$	31.6481	65.5	7.3	2.5	3.5	0.1	5.9	6.1
$C_{16}H_2$	36.5348	74.6	6.8	2.5	2.4	0.1	5.4	5.6
$C_{18}H_2$	41.4211	83.9	6.1	1.5	0.3	0.1	4.7	4.9

[a] The molecular length (L) is taken as the distance between the terminal carbon atoms in the optimized molecules. The percent difference is given by $\%\text{diff} = [\alpha_{CCSD(T)} - \alpha_i]\cdot 200/[\alpha_{CCSD(T)} + \alpha_i]$, where i = RHF, MP2, SCS-MP2, CCSD, B3LYP or PBE.

between the two can be attributed to the potential well in H_2^+, which is not infinitely steep at the boundaries of the quantum mechanical system. It is evident that the L^4 scaling of the polarizability also applies to simple three-dimensional molecular systems in which electron−electron repulsion is absent. Another interesting feature in the static polarizability of H_2^+ and H_2 is that the polarizability (α_{zz}) vertical to the internuclear axis is roughly constant and scales linearly with the internuclear hydrogen separation ($L^{1.164}$ and $L^{1.056}$, respectively). This is expected since the "box" length in the z direction (and y direction) is roughly constant with respect to variation of the hydrogen−hydrogen bond length. Concerning the polarizability along the molecular axis (α_{xx}), the reduction of the polarizability length dependence from $L^{3.916}$ to $L^{2.056}$ can be attributed to the existence of electron−electron repulsion that is absent in the H_2^+ and present in H_2. In the subsequent section, we observe that in polyynes, which have a greater number of electrons in a given molecular length, the polarizability length dependence is significantly reduced. This of course is detrimental to the nonlinear polarizability characteristics of this molecular class. It is noted that the polarizability length-dependence of H_2 only applies for a small range of the H−H bond lengths (1.0−2.2 Å). This is explained by the breaking of the chemical bond between the hydrogens at large internuclear distances monitored by electron density difference plots between the molecular (H_2) and the atomic ($H^{\bullet}$) electron densities. This results in a decrease of the polarizability since the presence of the chemical bond generates a region of space, distant from the nuclei centers, that can easily accommodate electron density. Therefore the external electric field has a larger influence on this region of space (chemical bond) and can polarize the electronic charge distribution more efficiently.

B. Polyynes. ***(i) Optimized Molecular Geometries.*** Previous workers have found that computed polarizabilities of polyynes are sensitive to the single and triple carbon−carbon bond lengths used.[50] Consequently, in this study we have examined a series of basis sets for 1,3,5,7,9-decapentayne ($C_{10}H_2$) to determine the one that would result in convergence of the geometric parameters of $C_{10}H_2$ to within a thousandth of an angstrom. These results are tabulated in Table 1 and show that the cc-pVTZ basis set is sufficient to yield molecular geometries of aug-cc-pVQZ quality. Additionally, we briefly investigated the possible influence of core-valence correlation on the optimized geometries of C_4H_2 and C_6H_2, using Dunning's correlation-consistent polarized core-valence triple-ζ basis set[39] (cc-pcVTZ) and allowing all core orbitals to participate in the electron correlation computation. We observe that bond length differences due to inclusion of core orbitals in the optimizations are less than 0.0005 Å compared to cc-pVTZ optimizations, thus the computationally less expensive cc-pVTZ basis set was eventually used. In Table 2 we present the CCSD(T)/cc-pVTZ optimized geometries for C_2H_2 through $C_{18}H_2$. The bond length alternation ($\Delta\delta$) in an infinite polyyne chain approaches the value of 0.1276 Å, whereas $\Delta\delta$ close to the polyyne terminals was found to be 0.1523 Å. Recently, the bond length alternation of polyynes has been estimated to be 0.13 Å, in very good agreement with our present findings.[51] This range of bond length alterations is due to the edge effect caused by the finite size of these polyynes. The extrapolated single and triple carbon−carbon bond lengths in polymeric polyynes are 1.357 Å and 1.229 Å, respectively. Comparison of the CCSD(T)/cc-pVTZ optimized bond lengths to the existing gas phase experimental bond length data[52,53] of acetylene (C_2H_2) and 1,3-butadiyne (C_4H_2) shows excellent agreement (see Table 2).

(ii) Polarizability. All polyyne geometries in this work were optimized at the same level of theory at which subsequent polarizability calculations were carried out because of the sensitivity of the polarizability on the molecular geometry adopted.[50] As shown in the previous section, the optimized molecular structures of all polyynes exhibit a strong bond length alternating ($\Delta\delta$) character. The carbon−carbon framework alternates between triple (∼1.2172 Å) and single (∼1.3696 Å) carbon−carbon bonds. This phenomenon has been explained in terms of the first-order Peierls[54] distortion that result in $\Delta\delta$ and the formation of a significant bandgap at the Fermi level. Conjugated π-systems with a high degree of $\Delta\delta$ are considered semiconductors[55] in contrast to zero-bandgap π-conjugated molecules that have metallic properties. Previous studies have shown that the degree of $\Delta\delta$ will decrease the static longitudinal polarizability that is, however, considerably weaker than the

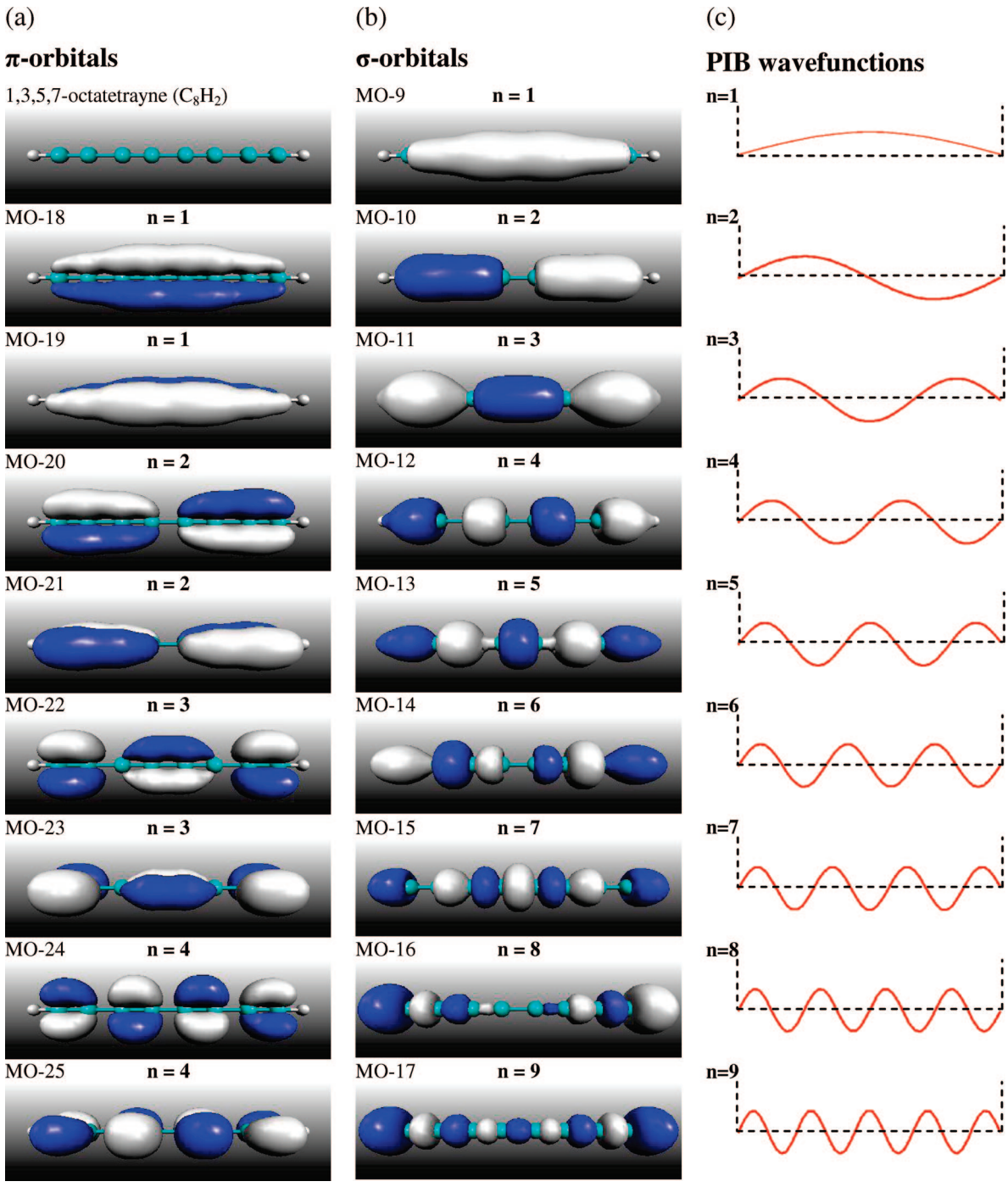

Figure 4. Two-electron wave function isosurfaces of 1,3,5,7-octaterayne (C_8H_2) and 1D-PIB. Three-dimensional isosurface of occupied (a) π-orbitals and (b) σ-orbitals of C_8H_2. (c) 1D-PIB wave functions for $n \leq 9$.

dependence on the length of the π-conjugated chain. Figure 3 shows the dependence of the static longitudinal and transverse polarizability as a function of the molecular length in polyynes.

The graphs exhibit a linear and nonlinear dependence of the transverse and longitudinal polarizability as a function of L. Both curves when fit by a power function of the form $a + b \cdot L^n$ yield an exponent n of 1.64 and 1.00, respectively. A similar value ($n = 1.5$) for the static longitudinal polarizability was found by Maroulis et al.[21] in smaller MW polyynes ($n \leq 4$). Static molecular polarizabilities are not directly comparable to experimental dynamic polarizabilities obtained from Kerr effect measurements, thus limited experimental measurements of static polarizabilities are available in the literature. Keir et al.[56] report values of 5.21, 3.21, 3.88 $\pm$ 0.08 ($10^{-40} \cdot C^2m^2J^2$) for the transverse, longitudinal, and molecular polarizability of acetylene (C_2H_2), respectively. We find at CCSD(T)/aug-cc-pVTZ//CCSD(T)/cc-pVTZ, values of 5.07, 3.11, 3.76 ($10^{-40} \cdot C^2m^2J^2$), respectively. Comparison of the experimental and theoretical values shows that this level of theory underestimates the experimental polarizabilities by only 3%. In order to study the performance of various methodologies in the assessment of polarizability compared to the higher-level coupled-cluster results, we obtained the optimized molecular geometries and polarizabilities for a wide range of methodologies (e.g., RHF, MP2, SCSMP2, CCSD, B3LYP, and PBE). In Table 3 we present the static longitudinal and transverse polarizability in polyynes with the various computational methods examined. The percent difference (%diff) is a measure of the agreement

between the various methods and the high-level CCSD(T) results. We observe that, for the longitudinal polarizability, RHF, MP2, SCSMP2, and CCSD perform well compared to CCSD(T), whereas commonly used DFT methods (B3LYP, PBE) considerably overestimate the polarizability, in some cases by 60%. This picture changes for the static transverse polarizability ($\alpha_{||}$) in polyynes where all methodologies seem to perform well to within 5−6% accuracy. This suggest that the polarizability errors that are present in DFT methods appear only along the molecular axis where errors introduced by the inaccurate description of the XC functionals are stronger due to increased orbital overlap.

The excellent performance of the RHF method in calculating polarizabilities with respect to the computationally intensive CCSD(T) method suggests that the decrease of the exponent cannot be attributed to electron correlation effects in contrast to first- and second-order hyperpolarizability computations where such effects were previously found to be important.[50] An asymptotic behavior of the polarizability per oligomer unit (α/n) as a function of the molecular length (L) is observed, especially for $\alpha_{\perp}$. This is in agreement with the findings of Kirtman and co-workers[57] who observe such an asymptotic behavior for the second-hyperpolarizabilities in PAs.

With the use of our highly accurate coupled-cluster results, we derive a quantitative structure−property relationship (QSPR) that that can be used as a predictive tool to obtain static longitudinal and transverse polarizabilities in polyynes as a function of their length (L). These relationships are

$$\alpha_{||} = (3.248 + 0.384L^{1.64}) \times 10^{-40}\ \mathrm{C^2m^2/J^2} \quad (7)$$

$$\alpha_{\perp} = (1.613 + 0.302L^{1.00}) \times 10^{-40}\ \mathrm{C^2m^2/J^2} \quad (8)$$

where L is the length between terminal carbon atoms. The relationships were obtained by fitting a second-order polynomial and a straight line to the longitudinal and transverse polarizability as a function of L, respectively. Subsequent use of the definition of the average static molecular polarizability yields

$$\alpha = (0.226L^2 + 6.526L + 11.784) \times 10^{-41}\ \mathrm{C^2m^2/J^2} \quad (9)$$

which can be used to predict the static molecular polarizability of oligomeric polyynes.

(iii) Wave Functions. To examine the underlying electronic structure of both polyynes and the 1D-PIB under the influence of an isotropic electric field, we obtained isosurfaces of the wave functions close to the Fermi level. The comparison reveals that there is a good correlation (Figure 4) between the wave function shape and relative energy in these two quantum mechanical systems. In particular, visual representations show that both valence σ- and π- orbitals in 1,3,5,7-octatetrayne (C_8H_2) have a 1:1 correspondence to the one-dimensional wave functions of the 1D-PIB, suggesting that the use of the 1D-PIB (previous section) to explain the polarizability trends in polyynes is valid. We observe in both quantum mechanical systems that the energy of the wave functions increases as a function of the number of nodes present and that the core, σ-, and π-electronic bands are completely separated in energy, with the first found at lower

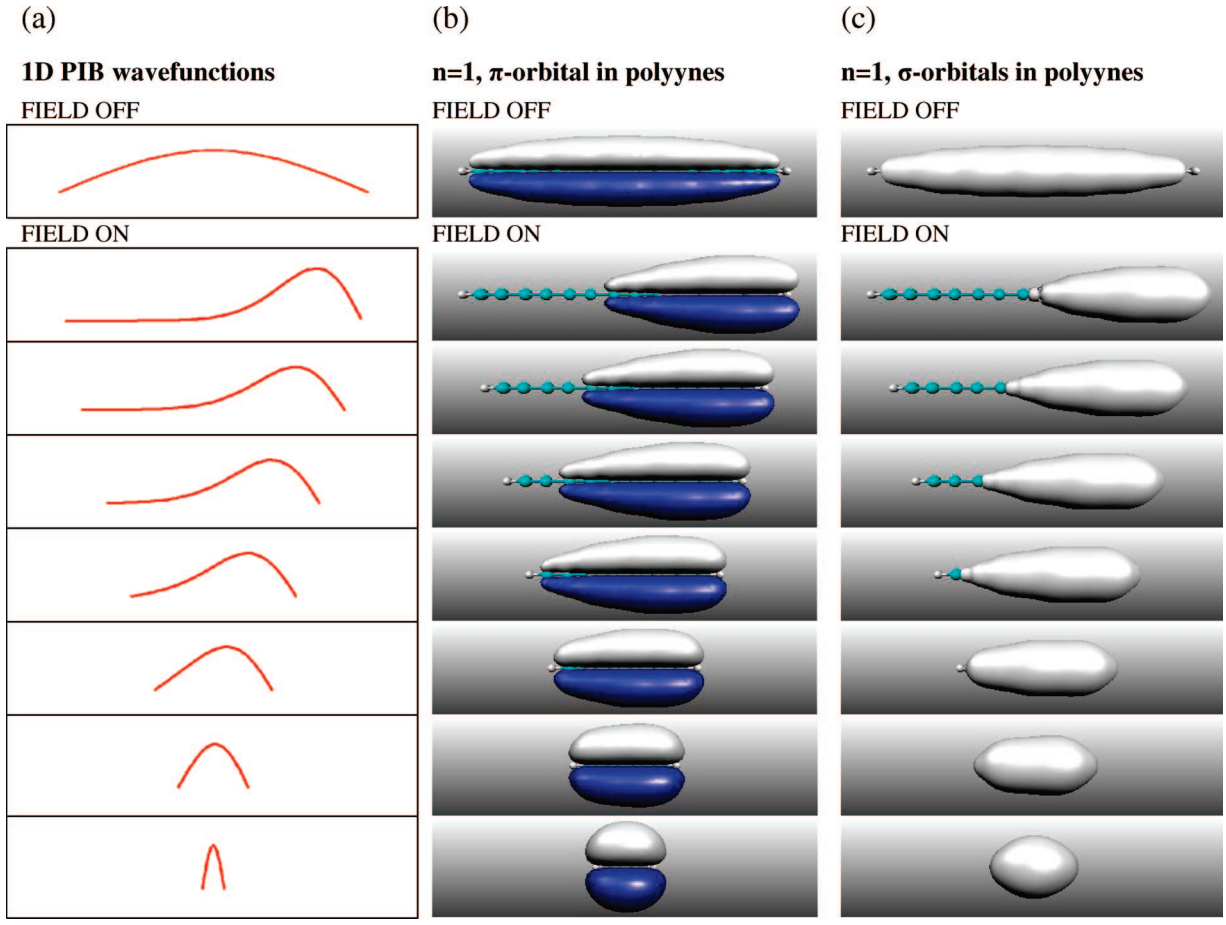

Figure 5. Isosurface of the $n = 1$ wave function in the (a) 1D-PIB, (b) π-orbitals, and (c) σ-orbitals of the homologous molecular sequence $C_{2n}H_2$. The electric field strength was set to 0.01 au to make the polarization of the orbitals visually more pronounced. Isosurfaces were obtained at a cutoff value of 0.01 au. For the PIB, the length (L) is set to the terminal carbon−terminal carbon separation of the corresponding polyyne.

energies. These molecules also have a considerably large bandgap that progressively decreases for higher MW polyynes. This suggests that polyynes are expected to be semiconductors regardless of their molecular length. In particular, at infinite chain length limit, our highly accurate CCSD(T)/cc-pVTZ optimizations showed a bond length alternation of 0.1276 Å in the center of polyynes.

To gain deeper insight into the length dependence of the polarizability, we also analyze the distortion of the molecular orbitals in polyynes due to the presence of an external electric field (Figure 5), and find that occupied states at the Fermi level in large MW polyynes exhibit increasingly larger distortions (polarization) in the presence of an external electric field than the corresponding states in smaller polyynes, indicative of their higher electron mobility.

It is evident that the influence of an electric field causes the $n = 1$, π- and σ-wave functions in the 1D-PIB and C_8H_2, respectively, to polarize in the direction of the positive end of the electric field. This behavior is in agreement with the fact that the negative charge of the electronic distribution is attracted by the positive end of the electric field. Furthermore, it can be seen that large distortions are present in the molecules of greater chain length. This result correlates well with the L^4 dependence of the longitudinal polarizability found earlier for the 1D-PIB. Increase of the polarizability as a function of polyyne length suggests the possibility of higher electron mobility along the longitudinal axis, which is attributed to the conjugated π-system. It should be noted that the effect of negative polarization was also observed in certain highly modulated wave functions. This effect is attributed to the orthogonality restriction imposed by the computations during wave function relaxations.

Conclusions

In this work we present QSPRs that predict the static longitudinal, transverse, and molecular polarizabilities in polyynes. Our systematic study of polarizabilities in polyynes and several one-dimensional quantum mechanical systems revealed that, in independent electron models, such as the 1D-PIB, 1D-SHO, and the molecular hydrogen cation (H_2^+), the polarizabilities scale as L^4, where L is the length of the model system. Such a strong length dependence is particularly desirable in the context of enhancing the nonlinear optical properties of linear polymeric materials. Nevertheless, in a multielectron molecular system, where electron−electron repulsions are present, the exponent of the polarizability length dependence is significantly weaker with adverse effects to the nonlinear optical properties. In particular, we show for the first time at the coupled-cluster level of theory that the static longitudinal polarizability scales as $L^{1.64}$, whereas for molecular hydrogen it scales as $L^{2.06}$. To provide an explanation for the exponent decrease, we carry out an extensive comparison of the polarizability calculated on various simple quantum mechanical systems that lack electron−electron repulsion as well as electron correlation and compare these to methods that take in account electron−electron repulsion (Hartree−Fock) and electron correlation (coupled-cluster). Our findings suggest that the exponent decrease is not a result of electron correlation effects but a result of electron−electron repulsion, in contrast to first- and second-order hyperpolarizability computations where electron correlation effects were previously found to be important.[50] Decrease of the electron−electron repulsion term is suggested to be the key term in enhancing nonlinear polarizability characteristics of linear polymeric materials.

Acknowledgment. We thank PURE Bioscience of El Cajon, California, for partial funding support of the computer resources. The authors acknowledge Professor Athanassios Nicolaides for useful discussions.

Appendix

Derivation of Eq 4: Analytic Polarizability for 1D-PIB

The expression of the second-order correction to the energy derived from nondegenerate time-independent perturbation theory is

$$E_n = \sum_{n\neq k} \frac{\langle \Psi_k^{(0)} | \hat{H}' | \Psi_n^{(0)} \rangle \langle \Psi_n^{(0)} | \hat{H}' | \Psi_k^{(0)} \rangle}{E_k^{(0)} - E_n^{(0)}} \tag{10}$$

where $\Psi_k^{(0)}$ and $\Psi_n^{(0)}$ are the zeroth-order wave functions, and $E_k^{(0)}$ and $E_n^{(0)}$ are the zeroth-order eigenvalues of the kth and nth energy levels, respectively. These for the 1D-PIB confined to a potential energy well that is zero between 0 and L ($0 < x < L$), but infinite outside that range are given by eqs 11 and 12.

$$\Psi^{(0)} = \sqrt{\frac{2}{L}} \cdot \sin\left(\frac{n\pi x}{L}\right) \tag{11}$$

$$E_n = \frac{n^2 h^2}{8 m_e L^2} \tag{12}$$

where $n = 1, 2, 3....$ The perturbation Hamiltonian in the x-direction is given by

$$\hat{H}' = \hat{\mu}_x \cdot E = -e \cdot E \cdot x \tag{13}$$

Substitution of the perturbation Hamiltonian into eq 10 yields the following expression for the second-order corrected energy of a wave function:

$$E_n^{(2)} = e^2 \cdot E^2 \sum_{n\neq k} \frac{\langle \Psi_k^{(0)} | \hat{x} | \Psi_n^{(0)} \rangle \langle \Psi_n^{(0)} | \hat{x} | \Psi_k^{(0)} \rangle}{E_k^{(0)} - E_n^{(0)}} \tag{14}$$

The bracket terms in this relationship after substituting the wave function of the 1D-PIB given in eq 11are evaluated as

$$\langle \Psi_k^{(0)} | \hat{H}' | \Psi_n^{(0)} \rangle = \langle \Psi_n^{(0)} | \hat{H}' | \Psi_k^{(0)} \rangle = \frac{2}{L} \int_0^L x \cdot \sin\left(\frac{n\pi x}{L}\right) \cdot \sin\left(\frac{k\pi x}{L}\right) dx \tag{15}$$

which, after symbolical evaluation and simplification, reduces to the following expression:

$$\langle \Psi_k^{(0)} | \hat{x} | \Psi_n^{(0)} \rangle = \frac{4 \cdot n \cdot k \cdot L[(-1)^{n+k} - 1]}{\pi^2 (n^2 - k^2)^2} \tag{16}$$

Hence the second-order corrected energy of a wave function for the simple 1D-PIB is given by substitution of eqs 12 and 16 into eq 14. This results in the following relationship:

$$E_n^{(2)} = e^2 \cdot E^2 \sum_{n\neq k} \frac{\left(\frac{4 \cdot n \cdot k \cdot L[(-1)^{n+k} - 1]}{\pi^2 (n^2 - k^2)^2}\right)^2}{\frac{k^2 h^2}{8 m_e L^2} - \frac{n^2 h^2}{8 m_e L^2}} \tag{17}$$

which, after a few algebraic steps, simplifies to

$$E_n = \frac{128 \cdot e^2 \cdot m_e \cdot L^4 \cdot E^2}{\pi^4 \cdot h^2} \sum_{n \neq k} \frac{n^2 \cdot k^2 [(-1)^{n+k} - 1]^2}{(n^2 - k^2)^5} \quad (18)$$

Using the second-order corrected energy of a wave function for the simple 1D-PIB, one can calculate the polarizability tensor x-component using the definition of polarizability given in eq 2. So the polarizability in the x-direction for the 1D-PIB is

$$\alpha_{xx} = \frac{-256 \cdot e^2 \cdot m_e \cdot L^4}{\pi^4 \cdot \hbar^2} \sum_{n \neq k} \frac{n^2 \cdot k^2 [(-1)^{n+k} - 1]^2}{(n^2 - k^2)^5} \quad (19)$$

where m_e is the electron mass, L is the length of the box, $\hbar$ is Planck's constant, e is the elementary charge of an electron, and n and k are the nth and kth energy levels, respectively.

Methodolgy in Section C: Numerical Polarizability of 1D-PIB with Sinusoidal Potential

Here we derive the equations required to numerically solve the 1D-PIB using the linear "shooting" method. Again the equation solved is the time-independent nonrelativistic Schrodinger equation, which for a single dimension is given by

$$-\frac{\hbar^2}{2m_e} \cdot \frac{d^2\Psi}{dx^2} + V\Psi = E\Psi \quad (20)$$

where $\hbar = h/2\pi$, and V is the potential under the influence of which electrons move. In the approach taken here, the potential is set equal to the sum of a sinusoidal potential generated by an array of nuclei (first term) and an isotropic homogeneous external electric field (second term) and is given by the expression

$$V = A \cdot \sin[2\pi(x + \phi)] - q \cdot E \cdot x \quad (21)$$

where A and φ are the amplitude and the phase of the sin-wave, respectively, and E is the electric field strength. The external electric field is used to study changes in the polarizability of the system. A combination of eqs 20 and 21 yields a second-order differential equation,

$$\frac{d^2\Psi}{dx^2} + \frac{2m_e}{\hbar^2}(E - A \cdot \sin[2\pi(x + \phi)] + q \cdot E \cdot x)\Psi = 0 \quad (22)$$

that needs to be solved numerically using the linear "shooting" method and the boundary condition in which the wave function vanishes at $x = 0$ and $x = L$.

The polarizability is given from the usual relationship,

$$\alpha = \frac{-\mu}{E} \quad (23)$$

where μ is the induced dipole moment given by the expression

$$\mu = \frac{\int_0^L \Psi^* \hat{x} \Psi d\tau}{\int_0^L \Psi^* \Psi d\tau} \quad (24)$$

Supporting Information Available: Polyyne bond lengths optimized using various theoretical methods such as RHF, MP2, SCSMP2, and B3LYP. This material is available free of charge via the Internet at http://pubs.acs.org.

References and Notes

(1) London, F. *Z. Phys.* **1930**, *63*, 245.
(2) Zeinalipour-Yazdi, C. D.; Pullman, D. P. *J. Phys. Chem. B* **2006**, *110*, 24260.
(3) Zeinalipour-Yazdi, C. D. Electronic structure and interlayer binding energy of graphite. Ph.D. Thesis, University of California San Diego and San Diego State University, 2006.
(4) Hanna, D. C.; Yuratich, M. A.; Cotter, D. *Nonlinear Optics of Atoms and Molecules*; Springer: Berlin, 1979.
(5) Lane, N. F. *Rev. Mod. Phys.* **1980**, *52*, 29.
(6) Hohm, U. *J. Chem. Phys.* **1994**, *101*, 6362.
(7) Lecours, S. M.; Guan, H. W.; Dimagno, S. G.; Wang, C. H.; Therien, M. J. *J. Am. Chem. Soc.* **1996**, *118*, 1497.
(8) Vela, A.; Gázquez, J. L. *J. Am. Chem. Soc.* **1990**, *112*, 1490.
(9) Nagle, J. K. *J. Am. Chem. Soc.* **1990**, *112*, 4741.
(10) Champagne, B.; André, J.-M. *Int. J. Quantum Chem.* **1992**, *42*, 1009.
(11) Galiatsatos, V.; Neaffer, R. O.; Sen, S.; Sherman, R. J. *Physical Properties of Polymers Handbook*; AIP Press: Woodbury, NY, 1996.
(12) Zhou, M. *Opt. Eng.* **2002**, *41*, 1631.
(13) Jang, C.; Chen, R. T. *J. Lightware Technol.* **2003**, *21*, 1053.
(14) Ahn, S.; Shin, S. J. *Sel. Top. Quantum Electron.* **2001**, *7*, 819.
(15) Ma, C.; Zhang, H.; Zhang, D.; Cui, Z.; Liu, S. *Opt. Commun.* **2004**, *241*, 321.
(16) Champagne, B.; Fripiat, J. G.; Andre, J.-M. *J. Chem. Phys.* **1992**, *96*, 8330.
(17) Jaszunski, M.; Jorgensen, P.; Koch, H.; Agren, H.; Helgaker, T. *J. Chem. Phys.* **1993**, *98*, 7229.
(18) van Faassen, M.; de Boeij, P. L.; van Leeuwen, R.; Berger, J. A.; Snijders, J. G. *J. Chem. Phys.* **2003**, *118*, 1044.
(19) Champagne, B.; Öhrn, Y. *Chem. Phys. Lett.* **1994**, *217*, 551.
(20) Chopra, P.; Carlacci, L.; King, H. F.; Prasad, P. N. *J. Phys. Chem. A* **1989**, *93*, 7120.
(21) Maroulis, G.; Thakkar, A. J. *J. Chem. Phys.* **1991**, *95*, 9060.
(22) Archibong, E. F.; Thakkar, A. J. *J. Chem. Phys.* **1993**, *98*, 8324.
(23) Nalwa, H. S.; Mukai, J.; Kakuta, A. *J. Phys. Chem. A* **1995**, *99*, 10766.
(24) Jacquemin, D.; Champagne, B.; Andre, J. M. *Int. J. Quantum Chem.* **1997**, *65*, 679.
(25) Champagne, B.; Perpète, E. A.; van Gisbergen, S. J. A.; Baerends, E. J.; Snijders, J. G.; Ghaoui, C. S.; Robins, K. A.; Kirtman, B. *J. Chem. Phys.* **1998**, *109*, 10489.
(26) Kirtman, B.; Champagne, B.; Gu, F. L.; Bishop, D. M. *Int. J. Quantum Chem.* **2002**, *90*, 709.
(27) Paula, M.-S.; Qin, W.; Weitao, Y. *J. Chem. Phys.* **2003**, *119*, 11001.
(28) Poulsena, T. D.; Mikkelsen, K. V.; Fripiat, J. G.; Jacquemin, D.; Champagne, B. *J. Chem. Phys.* **2001**, *114*, 5917.
(29) Gu, F. L.; Bishop, D. M.; Kirtman, B. *J. Chem. Phys.* **2001**, *115*, 10548.
(30) Martinez, A.; Otto, P.; Ladik, J. *Int. J. Quantum Chem.* **2003**, *94*, 251.
(31) Kudin, K. N.; Scuseria, G. E. *J. Chem. Phys.* **2000**, *113*, 7779.
(32) Seminario, J. M.; de la Cruz, C.; Derosa, P. A.; Yan, L. *J. Phys. Chem. B* **2004**, *108*, 17879.
(33) Slepkov, A. D.; Hegmann, F. A.; Eisler, S.; Elliott, E.; Tykwinski, R. R. *J. Chem. Phys.* **2004**, *120*, 6807.
(34) Szafert, S.; Gladysz, J. A. *Chem. Rev.* **2003**, *103*, 4175.
(35) Jacquemin, D.; Champagne, B.; André, J.-M. *Int. J. Quantum Chem.* **1997**, *65*, 679.
(36) Sim, F.; Chin, S.; Dupuis, M.; Rice, J. E. *J. Phys. Chem.* **1993**, *97*, 1158.
(37) Dalskov, E. K.; Oddershede, J.; Bishop, D. M. *J. Chem. Phys.* **1998**, *108*, 2152.
(38) Pople, J. A.; McIver, J. W.; Ostlund, N. S. *J. Chem. Phys.* **1968**, *49*, 2965.
(39) Dunning, T. H., Jr. *J. Chem. Phys.* **1989**, *90*, 1007.
(40) Werner, H.-J.; Knowles, P. J., Lindh, R.; Manby, F. R.; Schütz, M.; Celani, P.; Korona, T.; Rauhut, G.; Amos, R. D.; Bernhardsson, A.; Berning, A.; Cooper, D. L.; Deegan, M. J. O.; Dobbyn, A. J.; Eckert, F.; Hampel, C.; Hetzer, G.; Lloyd, A. W.; McNicholas, S. J.; Meyer W.; Mura, M. E.; Nicklass, A.; Palmieri, P.; Pitzer, R.; Schumann, U.; Stoll, H.; Stone, A. J.; Tarroni, R.; Thorsteinsson, T. *MOLPRO, version 2006.1: A Package of Ab Initio Programs*; University of Birmingham: Birmingham, 2006.
(41) Frisch, M. J.; Trucks, G. W.; Schlegel, H. B.; Scuseria, G. E.; Robb, M. A.; Cheeseman, J. R.; Montgomery, J. A., Jr.; Vreven, T.; Kudin, K. N.; Burant, J. C.; Millam, J. M.; Iyengar, S. S.; Tomasi, J.; Barone, V.; Mennucci, B.; Cossi, M.; Scalmani, G.; Rega, N.; Petersson, G. A.; Nakatsuji, H.; Hada, M.; Ehara, M.; Toyota, K.; Fukuda, R.; Hasegawa, J.; Ishida, M.; Nakajima, T.; Honda, Y.; Kitao, O.; Nakai, H.; Klene, M.; Li, X.; Knox, J. E.; Hratchian, H. P.; Cross, J. B.; Bakken, V.; Adamo, C.; Jaramillo, J.; Gomperts, R.; Stratmann, R. E.; Yazyev, O.; Austin, A. J.; Cammi, R.; Pomelli, C.; Ochterski, J. W.; Ayala, P. Y.; Morokuma, K.; Voth, G. A.; Salvador, P.; Dannenberg, J. J.; Zakrzewski, V. G.; Dapprich, S.; Daniels, A. D.; Strain, M. C.; Farkas, O.; Malick, D. K.; Rabuck, A. D.; Raghavachari, K.; Foresman, J. B.; Ortiz, J. V.; Cui, Q.; Baboul, A. G.;

Clifford, S.; Cioslowski, J.; Stefanov, B. B.; Liu, G.; Liashenko, A.; Piskorz, P.; Komaromi, I.; Martin, R. L.; Fox, D. J.; Keith, T.; Al-Laham, M. A.; Peng, C. Y.; Nanayakkara, A.; Challacombe, M.; Gill, P. M. W.; Johnson, B.; Chen, W.; Wong, M. W.; Gonzalez, C.; Pople, J. A. *Gaussian 03*, revision C.02; Gaussian Inc.: Wallingford, CT, 2004.

(42) Grimme, S. *J. Chem. Phys.* **2003**, *118*, 9095.

(43) Press, W. H.; Teukolsky, S. A.; Vetterling, W. T.; Flannery, B. P. *Numerical Recipes in C++*, 2nd ed.; Cambridge University Press: Cambridge, U.K., 2002.

(44) Monagan, M. B.; Geddes, K. O.; Heal, K. M.; Labahn, G.; Vorkoetter, S. M.; McCarron, J.; DeMarco, P. *Maple 9.0*Maplesoft: Waterloo, Ontario, 2003.

(45) Arrighini, G. P.; Durante, N.; Guidotti, C.; Lamanna, U. T. *Theor. Chem. Acc.* **2000**, *104*, 327.

(46) Matsuura, M.; Kamizato, T. *Phys. Rev. B* **1986**, *33*, 8385.

(47) Atkins, P. W.; Friedman, R. S. *Molecular Quantum Mechanics*, 3rd ed.; Oxford University Press: Oxford, 1997.

(48) Rustagi, K. C.; Ducuing, J. *Opt. Commun.* **1974**, *10*, 258.

(49) Jr Morris, J. C. *Phys. Rev. B* **1928**, *32*, 456.

(50) Toto, J. L.; Toto, T. T.; de Melo, C. P.; Kirtman, B.; Robins, K. *J. Chem. Phys.* **1996**, *104*, 8586.

(51) Shujiang Yang, M. K. *J. Phys. Chem. A* **2006**, *110*, 9771.

(52) Botschwina, P. *Chem. Phys. Lett.* **1982**, *47*, 241.

(53) Goldstein, E.; Ma, B.; Li, J. H.; Allinger, N. L. *J. Phys. Org. Chem.* **1996**, *9*, 191.

(54) Peierls, R. *Quantum Theory of Solids*; Clarendon: Oxford, 1955.

(55) Abdurahman, A.; Shukla, A.; Dolg, M. *Phys. Rev. B* **2002**, *65*, 115106.

(56) Keir, R. I.; Lamb, D. W.; Ritchie, G. L. D.; Watson, J. N. *Chem. Phys. Lett.* **1997**, *279*, 22.

(57) Kirtman, B. *Int. J. Quantum Chem.* **1992**, *43*, 147.

JP800302S